Bangs, F., Welten, M., Davey, M. G., Fisher, M., Yin, Y., Downie, H., Paton, B., Baldock, R., Burt, D. W., & Tickle, C. (2010). Identification of genes downstream of the Shh signalling in the developing chick wing and syn-expressed with *Hoxd13* using microarray and 3D computational analysis. *Mechanisms of Development*, *127*(9-12), 428-441. https://doi.org/10.1016/j.mod.2010.08.001

Identification of genes downstream of the Shh signalling in the developing chick wing and syn-expressed with *Hoxd13* using microarray and 3D computational analysis

Fiona Bangs[1], Monique Welten[1], Megan G. Davey[2], Malcolm Fisher[3], Yili Yin[4], Helen Downie[1,5], Bob Paton[2], Richard Baldock[3], David W. Burt[2], and Cheryll Tickle[1,6]

[1]Department of Biology and Biochemistry, University of Bath, Bath BA2 7AY, United Kingdom;

[2]Department of Genetics and Genomics, The Roslin Institute and Royal (Dick) School of Veterinary Studies, The University of Edinburgh, Midlothian EH25 9PS, United Kingdom;

[3]MRC Human Genetics Unit, Western General Hospital, Crewe Road, Edinburgh EH4 2XU, Scotland, United Kingdom;

[4]Division of Cell and Developmental Biology, Wellcome Trust Biocentre, The University of Dundee, Dundee DD1 5EH, United Kingdom;

[5]SCRI, Invergowrie, Dundee, DD2 5DA, Scotland, United Kingdom

[6]Corresponding author. EMAIL: cat24@bath.ac.uk; FAX: +44 01225 386779

Short title: Shh regulated genes in the chick wing

Keywords: Sonic Hedgehog, Limb, *talpid*^{3}, Chicken, OPT, Microarray, *Hoxd13*, *Ptc1*.

Abstract

Sonic Hedgehog (Shh) signalling by the polarizing region at the posterior margin of the chick wing bud is pivotal in patterning the digits but apart from a few key downstream genes, such as *Hoxd13,* which is expressed in the posterior region of the wing that gives rise to the digits, the genes that mediate the response to Shh signalling are not known. To find genes that are co-expressed with *Hoxd13* in the posterior of chick wing buds and regulated in the same way, we used microarrays to compare gene expression between anterior and posterior thirds of wing buds from normal chick embryos and from polydactylous *talpid*^{3} mutant chick embryos, which have defective Shh signalling due to lack of primary cilia. We identified 1070 differentially expressed gene transcripts, which were then clustered. Two clusters contained genes predominantly expressed in posterior thirds of normal wing buds; in one cluster, genes including *Hoxd13*, were expressed at high levels in anterior and posterior thirds in *talpid*^{3} wing buds, in the other cluster, genes including *Ptc1,* were expressed at low levels in anterior and posterior thirds in *talpid*^{3} wing buds. Expression patterns of genes in these two clusters were validated in normal and *talpid*^{3} mutant wing buds by *in situ* hybridisation and demonstrated to be responsive to application of Shh. Expression of several genes in the *Hoxd13* cluster was also shown to be responsive to manipulation of protein kinase A (PKA) activity, thus demonstrating regulation by Gli repression. Genes in the *Hoxd13* cluster were then sub-clustered by computational comparison of 3D expression patterns in normal wing buds to produce syn-expression groups. *Hoxd13* and *Sall1* are syn-expressed in the posterior region of early chick wing buds together with 6 novel genes which are likely to be functionally related and represent secondary targets of Shh

signalling. Other groups of syn-expressed genes were also identified, including a group of genes involved in vascularisation.

Introduction

The formation of the digits of the chick wing is a classical model for investigating how a precise pattern of structures is generated during embryonic development. It is now well established that Sonic hedgehog (Shh) plays a pivotal role in specifying both the number of digits and the digit pattern but less is known about the downstream genes that mediate the response to Shh signalling, apart from a few key genes, 5'*Hox* genes including *Hoxd13*, together with *Tbx2* and *Tbx3* genes (Fromental-Ramain et al., 1996; Suzuki et al., 2004; Zakany et al., 2004). Here we have used microarrays together with analysis of 3D gene expression patterns to identify genes downstream of Shh signalling that are syn-expressed with *Hoxd13* in the chick wing bud and likely to represent genes functionally related to *Hoxd13* and involved in digit patterning.

The chick wing has three morphologically distinct digits, 2, 3 and 4 (running from anterior to posterior). All three digits arise from the posterior half of the early wing bud as shown by fate mapping experiments (Towers et al., 2008; Vargesson, 1997). A small region of cells at the posterior margin of the wing bud, now known as the polarizing region or zone of polarizing activity (ZPA), was found to act as an organizer and induce formation of an additional set of digits when grafted to the anterior margin of a second bud (Saunders and Gasseling, 1968; Tickle, 1981). The polarizing region expresses *Shh* (Riddle et al., 1993) and Shh protein diffuses into the adjacent region of the wing bud to set up a concentration gradient to specify antero-posterior positional values in a step-wise fashion. The positional values are then remembered and interpreted later when the digits develop to give each digit its particular morphology (Towers and Tickle, 2009). Shh also controls growth of the responding cells in the early bud and the region of the wing bud that gives rise to the digits expands about two-fold during the 24 hr period of pattern

specification. Growth is therefore an integral part of the patterning process and determines digit number (Towers et al., 2008). In the chick wing, Shh induces *Bmp2* expression and there is some evidence that Bmp2 signalling might act downstream of Shh and contribute to specifying antero-posterior positional values (Drossopoulou et al., 2000).

5'Hox genes have long been considered as candidates for encoding antero-posterior positional values in the early chick wing bud (Izpisua-Belmonte et al., 1991; Morgan et al., 1992). Application of Shh to the anterior margin of the early chick wing bud leads to induction of *5'Hox* gene expression (Yang et al., 1997) and misexpression of *Hoxd12* leads to changes in digit patterning. Genetic studies in mice however have revealed that the 5'*Hox* genes play multiple roles in vertebrate limb development, including an early role in establishing *Shh* expression in the polarizing region, and that *Hoxd13* and *Hoxa13* together are required for digit development (Zakany and Duboule, 2007). *Tbx2* and *Tbx3* have also been implicated in antero-posterior patterning with misexpression in developing chick legs leading to changes in digit patterning (Suzuki et al., 2004). In early chick wing buds, *Hoxd13* is expressed in the posterior distal region that is fated to form digits whereas *Tbx2* and *Tbx3* genes are expressed in two stripes, one posterior and one anterior.

We used the fact that *Hoxd13* expression defines the region of the early chick wing bud fated to form digits to design a microarray experiment in which we compared the transcriptional profiles of anterior and posterior thirds of chick wing buds to identify genes co-expressed with *Hoxd13* and therefore likely to be involved in digit patterning. *Hoxd13* is expressed in the posterior region of the chick wing because its expression is repressed anteriorly by Gli proteins, the transcriptional effectors of Shh signalling which

are processed on primary cilia to repressor forms, in the absence of Shh. Therefore to refine this analysis further, we also added a comparison with transcriptional profiles of anterior and posterior thirds of wing buds from the chicken *talpid*^{3} mutant, in which Gli processing cannot take place due to absence of primary cilia (Davey et al., 2006; Yin et al., 2009) and in which *Hoxd13* is expressed at high levels both posteriorly and anteriorly (Izpisua-Belmonte et al., 1992; Lewis et al., 1999). Other genes such as *Ptc1*, are also expressed posteriorly in normal wing buds due to processing of Gli to activator forms which also occurs on primary cilia in the presence of Shh. In *talpid*^{3} mutant wing buds *Ptc1* is expressed at very low levels. Thus comparing expression of "posterior genes" in the wing buds of *talpid*^{3} mutants provides a way of identifying posteriorly expressed genes that, like *Hoxd13*, are regulated by Gli repression.

We focussed on two clusters of genes identified by our microarrays, one cluster of genes expressed like *Hoxd13*, the other like *Ptc1*. We validated expression patterns in the wing buds of both normal and *talpid*^{3} mutant embryos via *in situ* hybridisation and then carried out functional analyses to demonstrate responsiveness to Shh for genes in both clusters. We also tested whether expression of a sample of genes from the *Hoxd13* cluster was regulated by Gli repression by blocking protein kinase A (PKA) activity in the anterior region of normal chick wing buds, which is required for phosphorylation of Gli proteins and Gli repressor formation (Tiecke et al., 2007). To further refine our search for *Hoxd13* syn-expressed genes we compared the 3D expression patterns of a cohort of mostly novel Shh responsive genes in the *Hoxd13* cluster and used previously described computational methods (Fisher et al., 2008) to cluster genes that were similarly expressed. Through this sub-clustering, we dissected out a small group of 6 genes syn-expressed with *Hoxd13* and predicted to be functionally related. We also identified other

groups of syn-expressed genes potentially involved in other processes, such as vascularisation.

Materials and Methods

Embryos

Fertilized White Leghorn chicken eggs were obtained from H. Stewart (Lincolnshire), incubated at 37°C and staged according to (Hamburger and Hamilton, 1951). *Talpid*^{3} carriers were maintained and genotyped as per Davey et al. (2006).

Collection of tissue and RNA extraction

Workspace and dissection tools were thoroughly cleaned using RNaseZap (Ambion), then rinsed in diethyl pyrocarbonate (depc, SIGMA) treated water. Stage HH24 embryos were dissected into fresh depc treated PBS. Wing buds were cut into thirds along the antero-posterior axis (See Fig. 2) then placed in RNAlater (Ambion). Normal anterior and posterior thirds were pooled into groups of 10 pieces, which yielded sufficient RNA (<500 ng/μl) to hybridise to a single Affymetrix gene expression chip, so no amplification was required. We used anterior and posterior thirds because this ensured that the two limb regions were discrete. *talpid*^{3} wing bud thirds were stored separately until genotypes were confirmed. RNA was extracted as per Affymetrix recommended protocol.

Microarray analysis

Relative levels of RNA transcripts were compared between anterior and posterior wing bud thirds using chicken Affymetrix chips. Data collected with Affymetrix scanner was normalized using the Plier algorithm within the expression console package from Affymetrix and log2 transformed. 5 replicates of anterior third normal wing buds, 4 replicates of posterior third of normal wing buds and 4 replicates each of anterior and

posterior thirds of *talpid*^{3} wing buds at stage HH24 were examined. Sets of differentially expressed genes between specific limb bud regions in normal and *talpid*^{3} mutant embryos were identified using Limma (http://bioinf.wehi.edu.au/limma/). A false discovery rate (FDR) of 5% was used. The data were then clustered using Chinese restaurant clustering (Qin, 2006) and visualised within the Genesis package (http://genome.tugraz.at/).

Whole mount RNA *in situ* hybridisation

Whole mount *in situ* hybridization was performed as per Wilkinson and Nieto 1993. For simultaneous detection of two transcripts, embryos were hybridised with dioxygenin, (DIG, Roche) and fluorescein (Roche) labelled probe. INT/BCIP (Roche) was used to detect the first probe then subsequently washed out using 100% methanol before the second probe was detected with NBT/BCIP (Roche).

Implantation of Shh soaked beads

Beads were prepared and implanted into the anterior of stage HH21 Normal embryos as per Tiecke et al., (2007). Embryos were incubated for 4-20 hours before fixing in 4% PFA, then gene expression analysed via in situ hybridisation.

Electroporation of presumptive limb

1 µg/µl dnPKA RCAS or RCAS:GFP construct and 1 µg/µl pCAGGs RFP + 0.2% fast green were injected into the coelom on right side of stage HH14 Normal embryos and a square wave current of 60 volts was applied for 50 milliseconds 5 times using a CUY21 Bex company electroporator (Tokyo). Embryos were then incubated for 48 hours. Those expressing RFP were fixed in 4% PFA and expression of viral protein and candidate gene were analysed via double in situ hybridisation.

OPT scanning, mapping and computational analysis

Embryos were processed as previously described (Fisher et al., 2008) and scanned with Bioptonics 3001 OPT scanner (www.bioptonics.com). Three replicates of each gene expression pattern were mapped onto a reference limb at corresponding stage (HH24) using Amira 4.1.1 software and a median expression pattern was calculated using Wlz software (Fisher et al., 2008). The reference limb was divided into non-overlapping subregions of 5 x 5 x 5 voxels or tiles giving a total of 2072 tiles using software from MRC HGU (Fisher et al., 2008). Each tile was used to calculate mean gene expression strength for each experimental gene expression pattern. Data were normalised by stretching the grey histogram for each 3D gene expression pattern to cover range from 0-255. A data set containing medians only and a data set containing total gene expression data (3 replicates for each gene, no medians) were imported in Tigr Multi experiment Viewer (TMeV, http://www.tm4.org/mev.html). Hierarchical clustering (Eisen et al., 1998) was applied using Pearson correlation with complete linkage to produce nested trees of 1) genes showing similar patterns and 2) tiles showing similar expression profiles. The number of clusters was determined by setting distance threshold to 50%. Both gene clusters and tile clusters (spatial domains) were then visualised using Amira 4.1.1 software (Ruthensteiner and Hess, 2008).

Results

Microarray analysis of gene expression in normal and *talpid*^{3} wing buds

Microarray analysis was used to compare gene expression across the antero-posterior axis of wing buds in normal and *talpid*^{3} mutant chicken embryos at stage HH24. 1070 differentially expressed transcripts were identified and clustered using Chinese Restaurant Clustering (Qin, 2006). This represents about 10% of genes expressed in the limb (Boardman et al., 2002). 16 clusters of genes with different expression profiles (Supp. Table 1) were obtained. We focussed on two clusters of genes expressed predominantly in the posterior of normal wing buds; cluster 6 containing 66 transcripts relating to 56 genes, including *Hoxd13*, expressed at high levels in anterior and posterior thirds of *talpid*^{3} mutant wing buds and predicted to be regulated by Gli repressor (Fig. 1A, B, C; Fig 2A, Class IV; Supp. Table 2) and cluster 5 containing 68 transcripts relating to 59 genes, including *Ptc1,* expressed at low levels in anterior and posterior thirds of *talpid*^{3} mutant wing buds and predicted to be regulated by Gli activator (Fig. 1D, E, F; Fig 2A, Class II; Supp. Table 3). Genes in the *Ptc1* cluster are thus analogous to Class II neural transcription factor genes (Fig. 2B). In addition, other clusters contained genes, including *Bmp4,* expressed predominantly in the anterior of normal wing buds and at high levels in anterior and posterior thirds of *talpid*^{3} mutant wing buds. Genes in the *Bmp4* cluster behave like the Class I neural transcription factor genes with *Bmp4* expression being normally limited to the anterior by Gli activator in the posterior promoting expression of an unknown repressor (Fig. 2A, Class I, B). Expression of other "anterior" genes, such as *Alx4*, could be due to Gli repressor in the anterior inhibiting expression of an unknown anterior repressor (Fig. 2A, Class III).

Analysis of the Gene Ontology annotation of the genes in the *Hoxd13* and *Ptc1* clusters is shown in Supp. Fig. 1. The categories with the largest number of genes are enzymes, signalling, which includes genes such as *Wnt5a* and *Bmp2* and transcription, which includes genes such as *N-Myc* involved in cell cycle regulation. Other categories included genes involved in angiogenesis, such as *Angiopoietin-2B (Ang2B)* and *Hypoxia inducible factor 1α (Hif1α)*. About 20% of the genes have no known function.

Validation of microarray data

The *Hoxd13* cluster contains 7 other genes previously shown to have similar expression profiles to *Hoxd13* in normal and *talpid*^{3} mutant wing buds i.e. *Hoxd12, Hoxd11, Bmp2, Ang2B, Vascular endothelial growth factor D (VEGF-D) Transducin-like enhancer of split 4 (TLE4)* and *N-Myc* (see refs Supp. Table 2). To validate expression patterns of the other genes in the two clusters, whole mount RNA *in situ* hybridisation in normal and *talpid*^{3} mutant chicken embryos at stage HH24 was carried out.

In the *Hoxd13* cluster, 69% of the genes (including those already known to be posteriorly expressed) were found to be expressed predominantly in the posterior third of normal wing buds (Fig. 3A and data not shown). Differences between levels of anterior and posterior expression of the remaining genes, for example *ADP-ribosylation-like factor homolog 6* (*Arl6*; data not shown) are either undistinguishable via *in situ* hybridisation, or expression is not detectable in the wing bud. Expression of some genes is not restricted to the posterior third of the wing bud but extends into the middle region, for example *Family with sequence similarity 101 B (FAM101B)* is expressed in a middle stripe (Fig. 3A arrows). In a few cases, expression was also seen in the ectoderm, for example *Notum* (Fig. 3A). Expression patterns sometimes differed between wing and leg

buds, thus *Lim only protein 1 (LMO1)*, is expressed in the posterior of the wing bud, but both posteriorly and anteriorly in the leg bud (data not shown).

92% of the "posterior" genes in the *Hoxd13* cluster are expressed at high levels across the entire antero-posterior axis of *talpid*^{3} mutant wing buds (Fig. 3A and data not shown, Supp. Table 2 red, orange, yellow and tan), while expression of the remaining genes was barely detectable in the wing bud, thus resembling an *Ptc1* expression profile (Supp. Table 2 green). *Ectoderm neural cortex 1 (ENC1)* is expressed throughout *talpid*^{3} wing buds (Fig. 3A) but no expression was detected in *talpid*^{3} leg buds (data not shown).

In the *Ptc1* cluster, 54% of the genes were found to be expressed predominantly in posterior thirds of normal wing buds. 31% of these "posterior" genes are expressed at very low levels in both anterior and posterior thirds of *talpid*^{3} mutant wing buds (Fig. 3B and data not shown; Supp. Table 3 red, orange and yellow), while, unexpectedly, 50% are expressed at high levels throughout *talpid*^{3} mutant wing buds, more like *Hoxd13* (Supp. Table 3 green; expression of 5 genes was the same in *talpid*^{3} as in wild-type; 1 gene was not tested; Supp. Table 3 blue and tan).

Although these *in situ* hybridization data generally confirm the microarray data, a few *Hoxd13*-like genes are expressed in a *Ptc1*-like pattern while many genes in the *Ptc1* cluster are expressed in a *Hoxd13*-like pattern. This overlap is due to the clustering algorithm, which determines the threshold expression levels that distinguish between genes in the two clusters.

Regulation of gene expression by Shh

To test directly whether expression of genes in the *Hoxd13* and *Ptc1* clusters in normal chick wing buds is responsive to Shh, beads soaked in 1 mg/ml Shh protein were

implanted into the anterior margin or middle of stage HH19/20 wing buds and gene expression analysed by *in situ* hybridisation after 16-20 hours (Yang et al., 1997). Beads soaked in PBS were used as a control and no change in *Hoxd13* expression was detected (11/11 cases).

9 genes in the *Hoxd13* cluster have already been shown to be responsive to Shh, including *Hoxd13, Bmp2* and *VEGF-D*, with ectopic gene expression being induced following Shh treatment (Supp. Table 2 see references). 19 other genes in the cluster were also found to be responsive to Shh (Fig. 4A and data not shown; Supp. Table 2 red, orange, yellow). High levels of ectopic expression of some genes, for example *Ubiquitin carboxyl-terminal hydrolase isozyme L1 (UCHL1)* were induced anteriorly by Shh (Fig. 4A), while for other genes, there is weaker induction, for example *FAM101B* (Fig. 4A).

Expression of 5 genes from the *Ptc1* cluster, *Ptc1* itself*, Phosphatidylinositol-specific phospholipase C, X domain containing 3 (PLC DX), Potassium voltage-gated channel subfamily H member 5 (KCNH5), SIX1, Synaptotagmin-9 (SYNT9-near)* was found to be induced in response to Shh (Fig. 4B and data not shown; Supp. Table 3, red) while expression of *Mu-type opioid receptor (OPRM1)* was not (Fig. 4B; Supp. Table 3 orange). The extent of the response was variable with expression of some genes, for example, *KCHN5* being induced all around the bead, while, in the case of *SYNT9-near*, posterior expression was extended more anteriorly. *Ptc1* is known to be a direct target of Gli activator and ectopic *Ptc1* expression has been shown to be induced in anterior mesenchyme as early as 4 hours following implantation of a Shh soaked bead (Drossopoulou et al., 2000). Ectopic expression of *PLC DX* was also induced after 4h exposure to Shh (1/2 cases) whereas *SYNT-near* was not (0/2 cases; Fig. 3C) suggesting that *PLC DX* may be a direct target of Gli activator.

These results show that expression of many genes in both clusters is regulated by Shh signalling as would be predicted from the changes in expression seen in *talpid*^{3} wing buds.

Regulation of expression of genes in the *Hoxd13* cluster by Gli repressor

To determine directly whether expression of genes in the *Hoxd13* cluster is negatively regulated by Gli3 repressor, we over-expressed dnPKA in the anterior region of normal wing buds, along with RFP, to control for transfection efficiency (Tiecke et al., 2007; see also Supp. Fig. 2A,B). Expression of *Hoxd13* was expanded anteriorly after dnPKA overexpression (5/5 cases, Fig. 5; over-expression of GFP acted as a control and *Hoxd13* expression was unaffected despite significant GFP expression, 5/5 cases; Supp. Fig. 2C-F). Expression of *LMO1, Scrapie-responsive protein 1 precursor (SCRG1), UCHL1, ENC1, notum, 1-acyl-sn-glycerol-3-phosphate acyltransferase epsilon (AGPAT5), Family with sequence similarity 49, member A (FAM49A)* and *Bmp2* was also increased in the anterior region of the wing bud after over-expression of dnPKA (Fig. 5; Supp. Table 2 red). In contrast, expression of *FAM101B* appeared to be reduced (Fig. 5) together with expression of *Rabphilin3A-like (DOC2A)* while expression of 3 other genes was unchanged (Supp. Table 2 yellow).

These results demonstrate that expression of *Hoxd13* and 8 out of the 13 other genes in the cluster tested is regulated by Gli repressor in the chick wing bud, validating our approach of using the expression pattern in *talpid*^{3} mutant wing bud to identify genes that are regulated by Gli repressor versus Gli activator.

Syn-expression groups within *Hoxd13* cluster

The precise expression patterns of genes within the *Hoxd13* cluster in normal wing buds varied with some patterns being more posteriorly restricted than others (Fig. 3). Therefore to sift out genes that are syn-expressed with *Hoxd13*, we compared 3D expression patterns of 26 genes in the *Hoxd13* cluster in normal wing buds, concentrating mostly on novel genes, 23 of which had been shown to be responsive to Shh. Whole mount *in situ* hybridization was carried out to give 3 replicate expression patterns for each of the 26 genes (*Shh* expression patterns were also added for comparison), the whole mounts were scanned using Optical Projection Tomography (Sharpe et al., 2002), the digital 3D spatial expression patterns obtained were mapped on to a reference wing bud at the corresponding stage using Amira software (Fisher et al 2008) and a median gene expression pattern for each gene was calculated. Quantitative comparisons were made by dividing the reference limb, with all the expression data mapped on to it, into 5x5x5 voxels giving a total of 2072 'tiles' (see Materials and Methods); and the mean gene expression strength in each tile was calculated for each experimental gene expression pattern.

Figure 6 (Supp. Fig. 3) shows a heat map generated using median expression patterns of each gene and illustrates the number of genes with a mean expression value greater than 30 in each tile throughout the wing bud; red indicates where the highest number of genes is expressed and blue indicates where very few genes are expressed. The superimposition of dissection cuts on the heat map (Fig. 6A) shows that all the genes are expressed in the posterior third of the limb and none in the anterior third. Thus the 3D expression profiles produced by OPT from whole mount *in situ* hybridisation fit very well with the microarray expression profile. Many genes are also expressed in the middle third

of the limb, correlating with *in situ* hybridisation expression patterns (Fig. 3A). The heat map also reveals that many genes are expressed with a ventral bias (Fig. 6B-E).

Both data sets, the medians and the total gene expression data (3 replicates for each gene, no medians) were clustered using hierarchical clustering. This produced clusters of non-overlapping spatial domains, each expressing a unique set of genes, and clusters of genes with similar expression patterns. 23 spatial clusters were generated from the median data set (Fig. 7, rows; 3 spatial clusters showed expression artefacts outside the limb and were omitted from further analysis; also see Supp. Fig. 4, Supp. Table 4 and 5). 7 gene clusters were generated from the median data set (Fig. 7 columns, Fig. 8; also see Supp. Fig. 5, Supp. Table 6). In the total gene expression data set, the three replicates for each gene mostly clustered together showing that expression patterns were consistent (Supp. Fig. 5).

Four of the spatial clusters, 9, 14, 19 and 22 contain *Hoxd13* (Table 1) and when added together recreate the complete *Hoxd13* expression pattern. Cluster 19 contains 21 genes, (Supp Fig. 6 green) is the most posteriorly restricted cluster of tiles at the tip of the wing bud and the only cluster to include *Shh*. Cluster 19 is encircled by cluster 14, containing 23 genes, which forms a narrow ring of tiles more proximally (Fig.6 yellow). Cluster 9 contains 24 genes, (Supp. Fig.6 purple) is posterior but further proximal and ventral to cluster 14. Cluster 22 containing 23 genes, (Supp Fig.6 pink) extends further proximally still and dorsally from cluster 9 and represents the faint "tail" of *Hoxd13* expression which extends proximally. Other more anterior spatial clusters are also present and contain smaller numbers of genes not including *Hoxd13*.

One of the 7 gene syn-expression groups contains *Hoxd13* and 6 other genes including *Sall1* (Supp. Fig. 7), 3 syn-expression groups contain 2-10 genes and 3 contain

only one gene (Fig. 8). Another syn-expression group contains *VEGF-D* and *FAM101B*, which both appear to be expressed in the main limb artery and *Ephrin type-B receptor 1 (EphB1;* Fig. 8). It should be noted that genes whose expression was induced anteriorly by dnPKA and therefore regulated by Gli repressor are represented in 5 of the 7 groups (Bold in Fig. 8).

Thus the computational analysis not only dissected out discrete domains of expression with, as expected, those containing *Hoxd13* being located in the posterior region of the wing bud, but also identified genes syn-expressed with *Hoxd13*.

Discussion

We have used microarrays to compare the transcriptional profiles of tissue from normal and mutant chick wing buds and identified 35 genes that are predominantly expressed in the posterior of chick wing buds like *Hoxd13* and regulated by Gli repressor. We have identified a further 10 genes also expressed in the posterior which are likely to be regulated by Gli activator as expression of these genes is lost in *talpid*^{3} mutant wing buds. Previous work comparing the genes expressed in the anterior of normal and Gli3 mutant mouse limb buds identified 17 genes differentially expressed, and one of these was Slug also identified in our analysis (McGlinn et al., 2005). More recently, Vokes et al. (2008) carried out a series of microarray comparisons between various normal and mutant mouse limb buds, including *Gli3* mutants, and sophisticated genetic experiments to find posterior genes directly regulated by Gli3 repressor. They identified 23 genes with a Gli binding site that showed very pronounced asymmetry in expression. Despite the species difference, tissue selection and stage of development (E11.5 mouse limb bud is more developmentally advanced than chick stage HH24 wing buds), 9 of the genes identified by Vokes et al., (2008) also featured in our analysis (Supp. Table 7), including 4 of the genes in our *Hoxd13* cluster, *Hoxd13* itself, *Sall, Hoxd11,* and *Bmp2* and 2 of the genes in our *Ptc1* cluster, *Ptc1* itself and *Hand2.* All of these 6 genes are already known to be involved in vertebrate limb development.

By clustering 3D expression patterns of genes in the *Hoxd13* cluster, we found 6 genes that are syn-expressed with *Hoxd13* at the posterior of the chick wing bud and potentially functionally related and involved in digit patterning. Interestingly, the product of another gene in this syn-expression group, *Sall1*, a gene also likely to be directly regulated by Gli repressor according to Vokes et. al., (2008) is known to interact with

Hoxd13 by competing for target binding sequences of *Hoxd13* target genes (Kawakami et al., 2009). The fact that two of the genes in this syn-expression group are already known to be functionally related validates our approach. Fig. 9 shows how our data can fit into the relevant part of the model for the cis-regulatory network underlying Gli-mediated limb patterning produced by Vokes et. al. (2008). Since our microarray analysis will identify both direct and indirect targets of Shh signalling, the other 5 syn-expressed genes in the group *TLE4, TCERG1L, SCRG1, CPXM2* and *FAM49A* are therefore predicted to be downstream of *Hoxd13* and/or *Sall1* and the next step will be to determine whether and how the syn-expressed genes interact.

Expression of one of these genes, *TLE4*, a member of the Groucho family, has been previously described in developing wing buds (Van Hateren et al., 2005) and *TLE4* and *TCERG1L* encode proteins that play roles in regulating gene transcription. TLE4 can function as a co-repressor and interact with a range of different DNA-binding proteins including those involved in mediating signalling pathways, including Notch, Wnt and Bmp (Buscarlet and Stifani, 2007). *SCRG1* encodes a secreted protein and is strongly expressed in articular cartilage (Ochi et al., 2006), while *CPXM2* encodes a novel metallocarboxypeptidase, although it is not clear whether it has enzymatic activity (Xin et al., 1998). There is no information about the function *FAM49A*, although both *FAM49A, TCERG1L* and *ENC1*, another gene in the *Hoxd13* cluster but not in this same syn-expression group, were all identified as being enriched in the dorsal horn of mouse embryonic spinal cord (Li et al., 2006).

Another posterior gene identified by the analyses of Vokes et. al. (2008) as being directly regulated by Gli and also came up in our analysis, although we have yet to put into a syn-expression group is *Bmp2*. In addition, Vokes et. al. (2008) also identified

Tbx2/3, genes already implicated in chick digit patterning but expressed both anteriorly and posteriorly and therefore would not be identified in our study. The identification of all these genes in developing vertebrate limbs reflects the striking parallels with *Drosophila* wing vein patterning (Tickle, 2006) where it is well-established that concentration-dependent signalling by Dpp (*Bmp2* homolog) signalling downstream of Hh controls expression of *Omb* (*Tbx2/3* homolog) and *Spalt* (*Sall1* homolog) genes that encode positional information. In addition, it is interesting that Dpp signalling also suppresses expression of other sets of genes in wing vein patterning and that Groucho (TLE4 homolog) participates in this repression. Finally, it should be noted that mutations in *Hoxd13*, *Tbx3*, *Sall1*, *Sall4* have also been associated with human conditions in which digit patterning is affected.

Another syn-expression group includes genes known to be expressed in the vasculature*, VEGFD* and *Ephrin type-B receptor 1 (EphB1)* (Huynh-Do et al., 2002), thus highlighting the role of Shh in regulating the vasculature. *FAM101B,* apparently co-expressed with VEGFD in the main artery of the chick wing, has no known function and these results suggest that it could be involved in vascular development. This is further demonstrated in the *talpid*^{3} mutant which has a highly abnormal vasculture (Davey et al., 2007). Other syn-expressed genes include *Membrane metalloendopeptidase, LMO1* and *BH3 death domain agonist*, which have been functionally linked in lymphomas (Bai et al., 2004). *LMO1*, has a homolog in *Drosophila, dLMO* which negatively regulates activity of the LIM homeodomain transcription factor, Apterous (Zeng et al., 1998) in wing development. Interestingly, *LMO1* was recently identified as a potential *Hox* gene target in the hindbrain (Chambers et al., 2009).

Another gene in the *Hoxd13* cluster with a homolog in Drosophila is *Notum*, currently not an syn-expression group on its own because only the epithelial expression has been mapped. Notum was first discovered through its ability to modulate the gradient of Wingless across the *Drosophila* wing disc (Giraldez et al., 2002). More recently it has emerged that Notum, including mammalian Notum, cleaves the GPI anchor that attaches heparin sulphate proteoglycans to the cell surface (Traister et al., 2007). These proteoglycans not only regulate Wnt activity but also the activity of several signalling molecules including Hedgehog. Therefore regulation of Notum expression downstream of Shh signalling in the chick wing may represent a feedback mechanism to modulate Shh signalling.

A larger set of 205 genes identified by Vokes et al., (2008) included the gene encoding Arl6 or Bardet-Biedl syndrome 3 protein (BBS3) (Chiang et al., 2004), which was present in our *Hoxd13* cluster. Arl6 localises to ciliated cells in *C.elegans* (Fan et al., 2004) and it is intriguing that our analysis using *talpid*^{3} mutant embryos that lack primary cilia (Yin et al., 2009) predicts that *Arl6* is downstream of Shh signalling in the chick wing. *Arl6* is also another example of a common gene that has been identified in these studies of both chick and mouse embryos. This comparative approach should be powerful in identifying conserved genes downstream of the Shh signalling with fundamental roles in digit patterning.

Acknowledgments

This work was supported by grants from the Biotechnology and Biological Sciences Research Council CT and DB (joint grants) G20298 and G20297 supporting YY and MD

respectively, FB was supported by a BBSRC Studentship and grant BB/E014496/1 to CT, MW by grant BB/G00093X/1 to CT. CT and HD were supported by The Royal Society. We thank Ark Genomics funded by the BBSRC for supplying ESTs and microarray analysis.

Figure Legends:

Figure 1: Expression levels of genes in *Hoxd13* and *Ptc1* clusters

Whole mount *in situ* showing expression patterns of A) *Hoxd13* and D) *Ptc1* in normal and *talpid*^{3} wing buds. Dashed lines indicate location of dissections of tissue used for microarrays. Graphical representation of expression levels of genes in B) *Hoxd13* cluster, E) *Ptc1* cluster. Fold change given on Y axis, each condition represented 4 times, apart from normal anterior represented 5 times, along X axis. Average fold change in expression level shown by purple line. Heat map of genes in C) *Hoxd13* cluster, F) *Ptc1* cluster. Each condition given along the top and Affymetrix identification numbers listed on right-hand side representing all transcripts in the cluster. Expression level indicated by sliding scale where green is low, red is high. (WA= Normal anterior, WP= Normal posterior, TA= *talpid*^{3} anterior, TP= *talpid*^{3} posterior)

Figure 2: Classification of genes expressed in the chick wing according to how they are regulated by Shh signalling

A) Schematic showing 4 classes of gene expression in chick wing. Class I genes e.g. *Bmp4,* expressed predominantly in anterior normal wing buds but at high levels throughout *talpid*^{3} wing buds (Francis-West et al., 1995) due to lack of posterior Gli activator which normally promotes expression of unknown repressor; analogous to Class I neural transcription factors (shown in B). Class II genes e.g. *Ptc1*, expressed predominantly in posterior of normal wing buds but with no high level expression in *talpid*^{3} wing buds (Lewis et al., 1999) due to absence of Gli activator in posterior; analogous to Class II neural transcription factors (shown in B). Class III genes e.g. *Alx4* expressed predominantly in anterior normal wing buds but not expressed in *talpid*^{3} wing

buds (Davey M; unpublished observations) due to absence of anterior Gli repressor which normally inhibits expression of an unknown repressor. Class IV genes e.g. *Hoxd13* expressed predominantly in posterior normal wing buds but at high levels throughout *talpid*^{3} wing buds (Izpisua-Belmonte et al., 1992) due to absence of anterior Gli repressor.

Figure 3: Expression patterns of genes in *Hoxd13* and *Ptc1* clusters in stage HH24 normal and *talpid*^{3} mutant wing buds

Whole mount *in situ* hybridizations in normal and *talpid*^{3} mutant wing buds at stage HH24 showing expression of a sample of the genes identified by the microarrays in A) *Hoxd13* and B) *Ptc1* clusters. Gene name on left-hand side. All genes expressed in posterior of normal wing buds and either expressed throughout *talpid*^{3} wing (genes in *Hoxd13* cluster) or absent in *talpid*^{3} wing (genes in *Ptc1* cluster). In most cases, expression in the normal wing bud is restricted to posterior mesenchyme, but *FAM101B* is also expressed in stripe through middle of wing (arrows) and *Notum* expressed in apical ectodermal ridge.

Figure 4: Regulation of gene expression by Shh

Whole mount *in situ* hybridisation either A and B) 16-20 hours or C) 4 hours, after implantation of Shh-soaked bead to anterior or middle of right wing bud. Gene names on left-hand side. Compare right and left wing buds, arrows indicate ectopic gene expression; asterisks indicate location of bead.

Figure 5: Regulation of expression of genes in the *Hoxd13* cluster by dnPKA

Co-electroporation of dnPKA viral construct and RFP into presumptive right wing bud. Left hand column shows RFP expression, limb outlined with dashed white line. Whole mount *in situ* hybridsation shows change in gene expression (arrows), compare left and right wing buds. Expression of all genes is upregulated apart from *FAM101B,* which appears to be reduced.

Figure 6: Heat Map showing expression intensity of genes from *Hoxd13* cluster

Heatmap depicting expression of 26 genes from *Hoxd13* cluster and the *Shh* gene to show the number of genes expressed in different regions of reference wing bud. Red indicates all 27 genes expressed with a gradient red to blue indicating lower numbers of genes expressed, see scale (Ai). Highest number of genes expressed in distal posterior ventral region of wing bud (see also Supp. Fig. 3). A) Dorsal view, dashed lines indicate location of dissections of tissue used for microarrays. B) Ventral view; lines on wing bud depict planes of section for digital sections in C-E. C) digital section number 25, showing expression of genes in distal part of limb is slightly higher in ventral region (v). D) digital section number 35 through middle and E) number 50 through proximal region of wing bud showing expression of genes in ventral region (v) is higher than in dorsal region (d).

Figure 7: Hierarchical clustering of median expression pattern of genes from *Hoxd13* cluster

Matrix showing hierarchical clustering of median 3D expression of 26 genes from *Hoxd13* cluster and of the *Shh* gene. Each cell represents a 5 x 5 x 5 voxel spatial volume or 'tile' in HH24 reference limb and coloured according to mean signal intensity for a particular gene in a particular tile. Columns represent gene clusters; rows represent tile

clusters i.e. spatial domains. Posterior spatial domains depicted on right-hand side of each column (see also supp. Fig. 5).

Figure 8: Gene clusters of median 3D expression data

Seven gene clusters generated by Hierarchical clustering of median 3D expression patterns of 26 genes from the *Hoxd13* cluster and of the *Shh* gene. *Shh* clusters alone indicating no other gene has exactly the same expression pattern. Expression of genes in bold, is induced by over-expression of dnPKA demonstrating negative regulation by Gli repressor. Each cluster of genes depicted on right-hand side in 3D. *Only ectodermal expression of *Notum* was mapped in this analysis.

Figure 9: Gene regulatory network downstream of Shh

Gene regulatory network downstream of Shh in the limb (modified from Vokes et.al., 2008). Arrows originate from a gene that positively regulates the target where the arrow ends. Blunt ended lines originate from a gene that negatively regulates the target where the line ends. Solid lines are taken from a schematic in Vokes et. al., (2008). Dashed lines and highlighted genes are those identified in our study. Dashed lines indicate this regulation is not proven and may be indirect. Genes highlighted in green are primary targets and genes highlighted in blue are secondary targets, of Shh signalling identified in the *Hoxd13* cluster. Genes highlighted in pink are primary targets of Shh signalling identified in the *Ptc1* cluster, this includes HAND2 however HAND2 is expressed throughout the *talpid*^{3} wing bud indicating it is negatively regulated by Gli repressor as shown in Vokes et. al., (2008). Our data also shows that *Bmp2* expression is negatively regulated by Gli repressor, see red dotted line.

Supplemental Figures

Supp. Fig. 1

Pie chart showing percent of gene ontologies represented by genes identified in *Hoxd13* and *Ptc1* clusters.

Supp. Fig. 2

Effects of dnPKA expression on skeletal pattern and GFP controls. A and B) Alcian green staining of day 10 chick embryo A) control non-electroporated wing B) electroporated with dnPKA leads to a reduction in Gli repressor formation and formation of an extra digit 2 resulting in a digit pattern 2234. C-D) Co-electroporation of RCAS GFP and pCAGGs RFP into right wing bud. C) RFP expression, D) GFP expressed by virus, E) expression of viral marker GAG detected by *in situ* hybridisation, F) no change in *Hoxd13* expression between GFP infected right wing bud and non-infected left wing bud, therefore viral infection does not affect gene expression.

Supp. Fig. 3

Movie of heatmap depicting expression of 26 genes from *Hoxd13* cluster and *Shh* and showing number of genes expressed in different regions of reference wing bud. Red indicates high numbers of genes with a gradient to blue indicating lower numbers of genes, see scale. The highest number of genes is expressed in distal-posterior-ventral region of wing bud.

Supp. Fig. 4

Interactive 3D model showing spatial clusters from both total and median data sets.

Supp. Fig. 5

Hierarchical clustering of total data set and gene clusters. A) Sample of hierarchical clustering of each replicate gene expression pattern. In most cases 3 replicates cluster together. A total of 20 spatial clusters and 7 genes clusters were generated. B) 3D representation of 7 gene clusters.

Supp. Fig. 6

Movie showing spatial domain clusters 9 (purple), 14 (yellow), 19 (green) and 22 (pink) of median gene expression patterns from *Hoxd13* cluster. Each cluster contains *Hoxd13*. Clusters are spatially discrete and do not overlap.

Supp. Fig. 7

Movie of genes expressed in cluster 3 visualised on reference wing bud: *Hoxd13* (green), *Sall1* (yellow), *SCRG1* (blue) and *FAM49A* (white) appearing in sequence.

Tables

Table 1

Spatial expression clusters containing *Hoxd13* (blue) generated by Hierarchical clustering of median 3D expression data of 26 genes from *Hoxd13* cluster and of the *Shh* gene. Genes unique to clusters are highlighted in colour. Total number of gene in each cluster given below cluster number.

Supplemental Tables

Supp. Table 1

Lists all genes in each of 16 clusters.

Supp. Table 2

Genes in *Hoxd13* cluster in order of fold change of expression between normal and *talpid*^{3} descending from highest to smallest. Results of *in situ* hybridisation and functional tests are given in the right hand columns, N/T = not tested.

Supp. Table 3

Genes in *Ptc1* cluster in order of fold change of expression between Normal and *talpid*^{3} descending from highest to smallest. Results of *in situ* hybridisation and functional tests are given in the right hand columns, N/T = not tested.

Supp. Table 4

All spatial clusters generated by Hierarchical clustering of medians of 3D expression data of 27 genes.

Supp. Table 5

Spatial clusters generated by Hierarchical clustering of three replicates of 3D expression data of 27 genes.

Supp. Table 6

Gene clusters generated by Hierarchical clustering of 3 replicates of 3D expression data of 27 genes.

Supp. Table 7

Lists 23 genes identified by Vokes et.al. 2008 shown to have an occupied Gli binding site and expressed in E11.5 posterior mouse limb; shows which genes were also identified in

our study after cross checking all 1070 differentially expressed transcripts. Genes from same family are also indicated.

References:

(Vokes et al., 2008) (Dealy et al., 1993; Farrell and Munsterberg, 2000; Francis et al., 1994; Francis-West et al., 1995; Izpisua-Belmonte et al., 1992; Izpisua-Belmonte et al., 1991; Nelson, 1996; Riddle et al., 1993; Ros, 1997; Trelles et al., 2002)

Bai, M., Skyrlas, A., Agnantis, N.J., Kamina, S., Tsanou, E., Grepi, C., Galani, V. and Kanavaros, P. (2004). Diffuse large B-cell lymphomas with germinal center B-cell-like differentiation immunophenotypic profile are associated with high apoptotic index, high expression of the proapoptotic proteins bax, bak and bid and low expression of the antiapoptotic protein bcl-xl. *Mod Pathol* **17**, (7): 847-56.

Boardman, P.E., Sanz-Ezquerro, J., Overton, I.M., Burt, D.W., Bosch, E., Fong, W.T., Tickle, C., Brown, W.R., Wilson, S.A. and Hubbard, S.J. (2002). A comprehensive collection of chicken cDNAs. *Curr Biol* **12**, (22): 1965-9.

Buscarlet, M. and Stifani, S. (2007). The 'Marx' of Groucho on development and disease. *Trends Cell Biol* **17**, (7): 353-61.

Chambers, D., Wilson, L.J., Alfonsi, F., Hunter, E., Saxena, U., Blanc, E. and Lumsden, A. (2009). Rhombomere-specific analysis reveals the repertoire of genetic cues expressed across the developing hindbrain. *Neural Dev* **4**: 6.

Chiang, A.P., Nishimura, D., Searby, C., Elbedour, K., Carmi, R., Ferguson, A.L., Secrist, J., Braun, T., Casavant, T., Stone, E.M. and Sheffield, V.C. (2004). Comparative genomic analysis identifies an ADP-ribosylation factor-like gene as the cause of Bardet-Biedl syndrome (BBS3). *Am J Hum Genet* **75**, (3): 475-84.

Davey, M.G., James, J., Paton, I.R., Burt, D.W. and Tickle, C. (2007). Analysis of talpid3 and wild-type chicken embryos reveals roles for Hedgehog signalling in development of the limb bud vasculature. *Dev Biol* **301**, (1): 155-65.

Davey, M.G., Paton, I.R., Yin, Y., Schmidt, M., Bangs, F.K., Morrice, D.R., Smith, T.G., Buxton, P., Stamataki, D., Tanaka, M., Munsterberg, A.E., Briscoe, J., Tickle, C. and Burt, D.W. (2006). The chicken talpid3 gene encodes a novel protein essential for Hedgehog signaling. *Genes Dev* **20**, (10): 1365-77.

Dealy, C.N., Roth, A., Ferrari, D., Brown, A.M. and Kosher, R.A. (1993). Wnt-5a and Wnt-7a are expressed in the developing chick limb bud in a manner suggesting roles in pattern formation along the proximodistal and dorsoventral axes. *Mech Dev* **43**, (2-3): 175-86.

Drossopoulou, G., Lewis, K.E., Sanz-Ezquerro, J.J., Nikbakht, N., McMahon, A.P., Hofmann, C. and Tickle, C. (2000). A model for anteroposterior patterning of the vertebrate limb based on sequential long- and short-range Shh signalling and Bmp signalling. *Development* **127**, (7): 1337-48.

Eisen, M.B., Spellman, P.T., Brown, P.O. and Botstein, D. (1998). Cluster analysis and display of genome-wide expression patterns. *Proc Natl Acad Sci U S A* **95**, (25): 14863-8.

Fan, Y., Esmail, M.A., Ansley, S.J., Blacque, O.E., Boroevich, K., Ross, A.J., Moore, S.J., Badano, J.L., May-Simera, H., Compton, D.S., Green, J.S., Lewis, R.A., van Haelst, M.M., Parfrey, P.S., Baillie, D.L., Beales, P.L., Katsanis, N., Davidson, W.S. and Leroux, M.R. (2004). Mutations in a member of the Ras superfamily of small GTP-binding proteins causes Bardet-Biedl syndrome. *Nat Genet* **36**, (9): 989-93.

Farrell, E.R. and Munsterberg, A.E. (2000). csal1 is controlled by a combination of FGF and Wnt signals in developing limb buds. *Dev Biol* **225**, (2): 447-58.

Fisher, M.E., Clelland, A.K., Bain, A., Baldock, R.A., Murphy, P., Downie, H., Tickle, C., Davidson, D.R. and Buckland, R.A. (2008). Integrating technologies for comparing 3D gene expression domains in the developing chick limb. *Dev Biol* **317**, (1): 13-23.

Francis, P.H., Richardson, M.K., Brickell, P.M. and Tickle, C. (1994). Bone morphogenetic proteins and a signalling pathway that controls patterning in the developing chick limb. *Development* **120**, (1): 209-18.

Francis-West, P.H., Robertson, K.E., Ede, D.A., Rodriguez, C., Izpisua-Belmonte, J.C., Houston, B., Burt, D.W., Gribbin, C., Brickell, P.M. and Tickle, C. (1995). Expression of genes encoding bone morphogenetic proteins and sonic hedgehog in talpid (ta3) limb buds: their relationships in the signalling cascade involved in limb patterning. *Dev Dyn* **203**, (2): 187-97.

Fromental-Ramain, C., Warot, X., Messadecq, N., LeMeur, M., Dolle, P. and Chambon, P. (1996). Hoxa-13 and Hoxd-13 play a crucial role in the patterning of the limb autopod. *Development* **122**, (10): 2997-3011.

Giraldez, A.J., Copley, R.R. and Cohen, S.M. (2002). HSPG modification by the secreted enzyme Notum shapes the Wingless morphogen gradient. *Dev Cell* **2**, (5): 667-76.

Hamburger, H. and Hamilton, H.L. (1951). A series of normal stages in the development of the chick embryo. *J. Exp. Morphol.* **88**: 49-92.

Huynh-Do, U., Vindis, C., Liu, H., Cerretti, D.P., McGrew, J.T., Enriquez, M., Chen, J. and Daniel, T.O. (2002). Ephrin-B1 transduces signals to activate integrin-mediated migration, attachment and angiogenesis. *J Cell Sci* **115**, (Pt 15): 3073-81.

Izpisua-Belmonte, J.C., Ede, D.A., Tickle, C. and Duboule, D. (1992). The mis-expression of posterior Hox-4 genes in talpid (ta3) mutant wings correlates with the absence of anteroposterior polarity. *Development* **114**, (4): 959-63.

Izpisua-Belmonte, J.C., Tickle, C., Dolle, P., Wolpert, L. and Duboule, D. (1991). Expression of the homeobox Hox-4 genes and the specification of position in chick wing development. *Nature* **350**, (6319): 585-9.

Kawakami, Y., Uchiyama, Y., Rodriguez Esteban, C., Inenaga, T., Koyano-Nakagawa, N., Kawakami, H., Marti, M., Kmita, M., Monaghan-Nichols, P., Nishinakamura, R. and Izpisua Belmonte, J.C. (2009). Sall genes regulate region-specific morphogenesis in the mouse limb by modulating Hox activities. *Development* **136**, (4): 585-94.

Lewis, K.E., Drossopoulou, G., Paton, I.R., Morrice, D.R., Robertson, K.E., Burt, D.W., Ingham, P.W. and Tickle, C. (1999). Expression of ptc and gli genes in talpid3 suggests bifurcation in Shh pathway. *Development* **126**, (11): 2397-407.

Li, M.Z., Wang, J.S., Jiang, D.J., Xiang, C.X., Wang, F.Y., Zhang, K.H., Williams, P.R. and Chen, Z.F. (2006). Molecular mapping of developing dorsal horn-enriched genes by microarray and dorsal/ventral subtractive screening. *Dev Biol* **292**, (2): 555-64.

McGlinn, E., van Bueren, K.L., Fiorenza, S., Mo, R., Poh, A.M., Forrest, A., Soares, M.B., Bonaldo Mde, F., Grimmond, S., Hui, C.C., Wainwright, B. and Wicking, C. (2005). Pax9 and Jagged1 act downstream of Gli3 in vertebrate limb development. *Mech Dev* **122**, (11): 1218-33.

Morgan, B.A., Izpisua-Belmonte, J.C., Duboule, D. and Tabin, C.J. (1992). Targeted misexpression of Hox-4.6 in the avian limb bud causes apparent homeotic transformations. *Nature* **358**, (6383): 236-9.

Nelson, C.E., Morgan, B.A., Burke, A.C., Laufer, E., DiMambro, E., Murtaugh, C., Gonzalez, E., Tessarollo, L., Parada, L.F., and Tabin, C. (1996). Analysis of Hox gene expression in the chick limb bud. *Development.* **122**: 1449-1466.

Ochi, K., Derfoul, A. and Tuan, R.S. (2006). A predominantly articular cartilage-associated gene, SCRG1, is induced by glucocorticoid and stimulates chondrogenesis in vitro. *Osteoarthritis Cartilage* **14**, (1): 30-8.

Qin, Z.S. (2006). Clustering microarray gene expression data using weighted Chinese restaurant process. *Bioinformatics* **22**, (16): 1988-97.

Riddle, R.D., Johnson, R.L., Laufer, E. and Tabin, C. (1993). Sonic hedgehog mediates the polarizing activity of the ZPA. *Cell* **75**, (7): 1401-16.

Ros, M.A., Sefton, M. and Nieto, A. (1997). Slug, a zinc finger gene previously implicated in early patterning of the mesoderm and neural crest, is also involved in chick limb development. *Development* **124**: 1821-1829.

Ruthensteiner, B. and Hess, M. (2008). Embedding 3D models of biological specimens in PDF publications. *Microsc Res Tech* **71**, (11): 778-86.

Saunders, J.W. and Gasseling, M.T. (1968). *Ectodermal-mesenchymal interactions in the origin of limb symmetry*. Epithelial-mesenchymal interactions. Fleischmeyer, R. and Billingham, R.E. Baltimore, Williams & Wilkins: 78-97.

Sharpe, J., Ahlgren, U., Perry, P., Hill, B., Ross, A., Hecksher-Sorensen, J., Baldock, R. and Davidson, D. (2002). Optical projection tomography as a tool for 3D microscopy and gene expression studies. *Science* **296**, (5567): 541-5.

Suzuki, T., Takeuchi, J., Koshiba-Takeuchi, K. and Ogura, T. (2004). Tbx Genes Specify Posterior Digit Identity through Shh and BMP Signaling. *Dev Cell* **6**, (1): 43-53.

Tickle, C. (1981). The number of polarizing region cells required to specify additional digits in the developing chick wing. *Nature* **289**, (5795): 295-8.

Tickle, C. (2006). Making digit patterns in the vertebrate limb. *Nat Rev Mol Cell Biol* **7**, (1): 45-53.

Tiecke, E., Turner, R., Sanz-Ezquerro, J.J., Warner, A. and Tickle, C. (2007). Manipulations of PKA in chick limb development reveal roles in digit patterning including a positive role in Sonic Hedgehog signaling. *Dev Biol* **305**, (1): 312-24.

Towers, M., Mahood, R., Yin, Y. and Tickle, C. (2008). Integration of growth and specification in chick wing digit-patterning. *Nature* **452**, (7189): 882-6.

Towers, M. and Tickle, C. (2009). Generation of pattern and form in the developing limb. *Int J Dev Biol* **53**, (5-6): 805-12.

Traister, A., Shi, W. and Filmus, J. (2007). Mammalian Notum induces the release of glypicans and other GPI-anchored proteins from the cell surface. *Biochem J*.

Trelles, R.D., Leon, J.R., Kawakami, Y., Simoes, S. and Izpisua Belmonte, J.C. (2002). Expression of the chick vascular endothelial growth factor D gene during limb development. *Mech Dev* **116**, (1-2): 239-42.

Van Hateren, N., Belsham, A., Randall, V. and Borycki, A.G. (2005). Expression of avian Groucho-related genes (Grgs) during embryonic development. *Gene Expr Patterns* **5**, (6): 817-23.

Vargesson, N., Clarke, J.D.W., Vincent, K., Coles, C., Wolpert, L., and Tickle, C. (1997). Cell fate in the chick limb bud and relationship to gene expression. *Development.* **124**: 1909-1918.

Vokes, S.A., Ji, H., Wong, W.H. and McMahon, A.P. (2008). A genome-scale analysis of the cis-regulatory circuitry underlying sonic hedgehog-mediated patterning of the mammalian limb. *Genes Dev* **22**, (19): 2651-63.

Xin, X., Day, R., Dong, W., Lei, Y. and Fricker, L.D. (1998). Identification of mouse CPX-2, a novel member of the metallocarboxypeptidase gene family: cDNA cloning, mRNA distribution, and protein expression and characterization. *DNA Cell Biol* **17**, (10): 897-909.

Yang, Y., Drossopoulou, G., Chuang, P.T., Duprez, D., Marti, E., Bumcrot, D., Vargesson, N., Clarke, J., Niswander, L., McMahon, A. and Tickle, C. (1997). Relationship between dose, distance and time in Sonic Hedgehog-mediated regulation of anteroposterior polarity in the chick limb. *Development* **124**, (21): 4393-404.

Yin, Y., Bangs, F., Paton, I.R., Prescott, A., James, J., Davey, M.G., Whitley, P., Genikhovich, G., Technau, U., Burt, D.W. and Tickle, C. (2009). The Talpid3 gene (KIAA0586) encodes a centrosomal protein that is essential for primary cilia formation. *Development* **136**, (4): 655-64.

Zakany, J. and Duboule, D. (2007). The role of Hox genes during vertebrate limb development. *Curr Opin Genet Dev* **17**, (4): 359-66.

Zakany, J., Kmita, M. and Duboule, D. (2004). A dual role for Hox genes in limb anterior-posterior asymmetry. *Science* **304**: 1669-1672.

Zeng, C., Justice, N.J., Abdelilah, S., Chan, Y.M., Jan, L.Y. and Jan, Y.N. (1998). The Drosophila LIM-only gene, dLMO, is mutated in Beadex alleles and might represent an evolutionarily conserved function in appendage development. *Proc Natl Acad Sci U S A* **95**, (18): 10637-42.

Figure 1

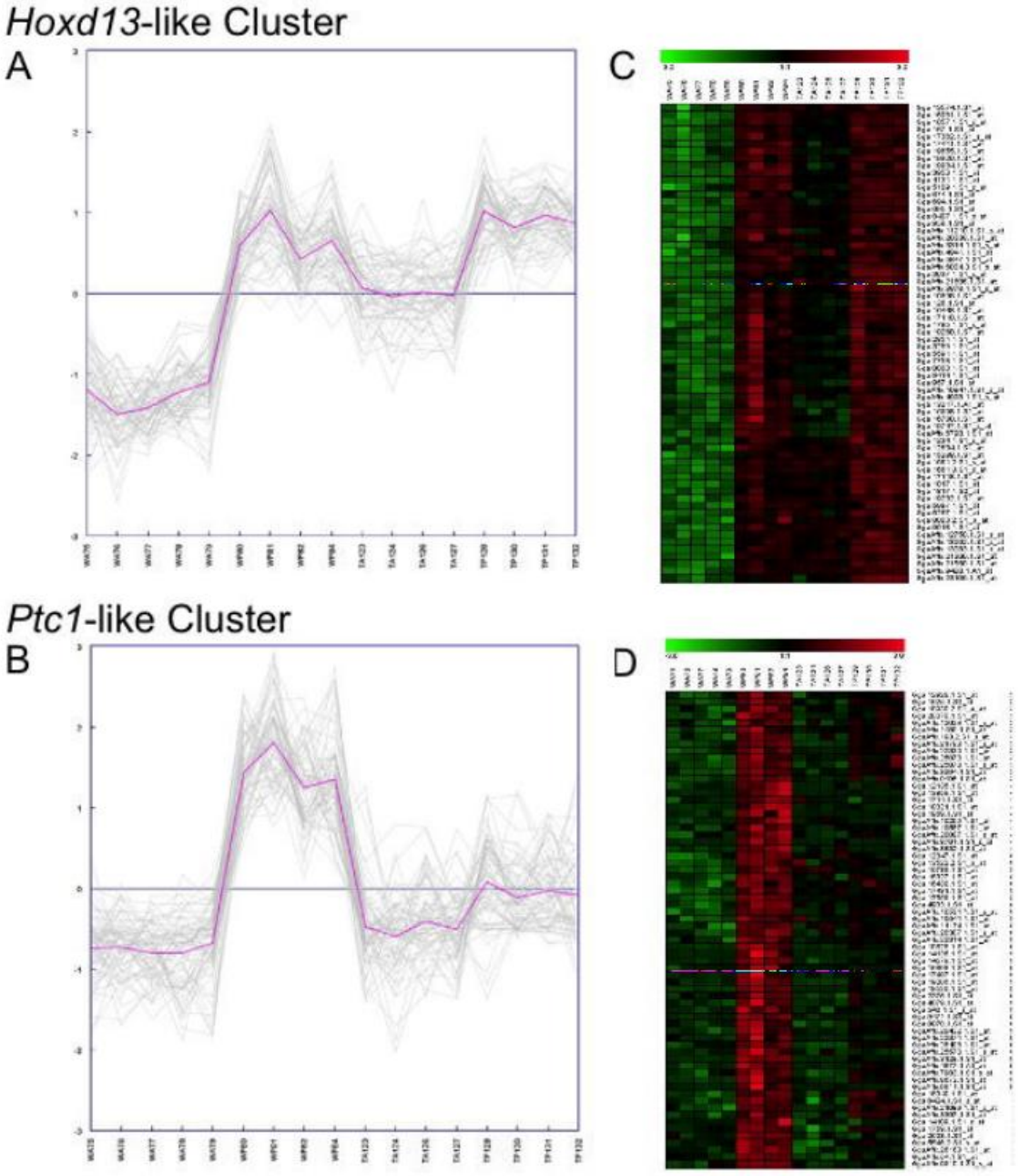

Figure 2

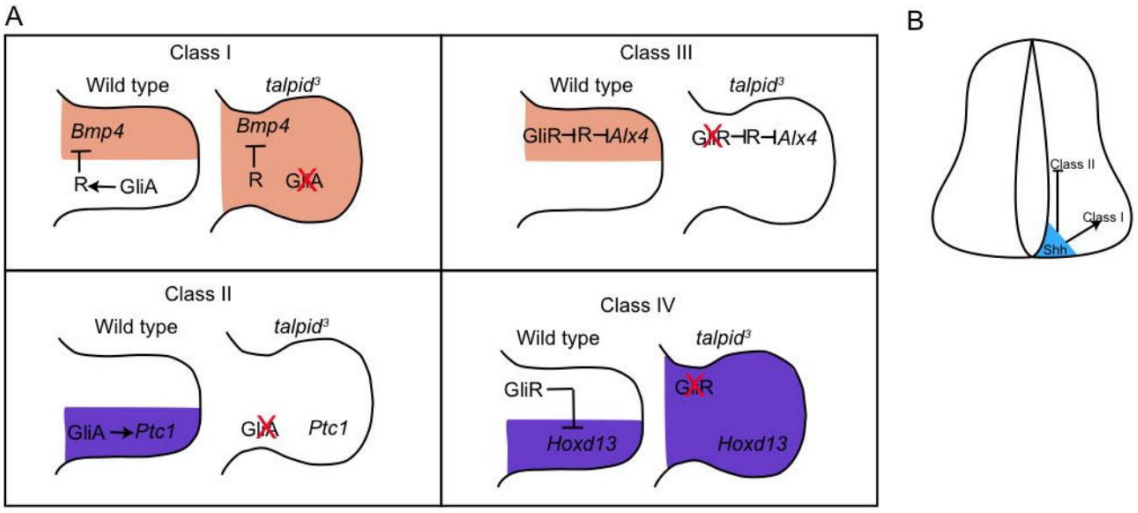
A
Class I
Wild type
talpid3
Bmp4
R
GliA
Bmp4
R
GliA
Class III
Wild type
talpid3
GliR
IR
Alx4
GliR
IR
Alx4
Class II
Wild type
talpid3
GliA
Ptc1
GliA
Ptc1
Class IV
Wild type
talpid3
GliR
Hoxd13
GliR
Hoxd13
B
Class II
Class I
Shh

Figure 3

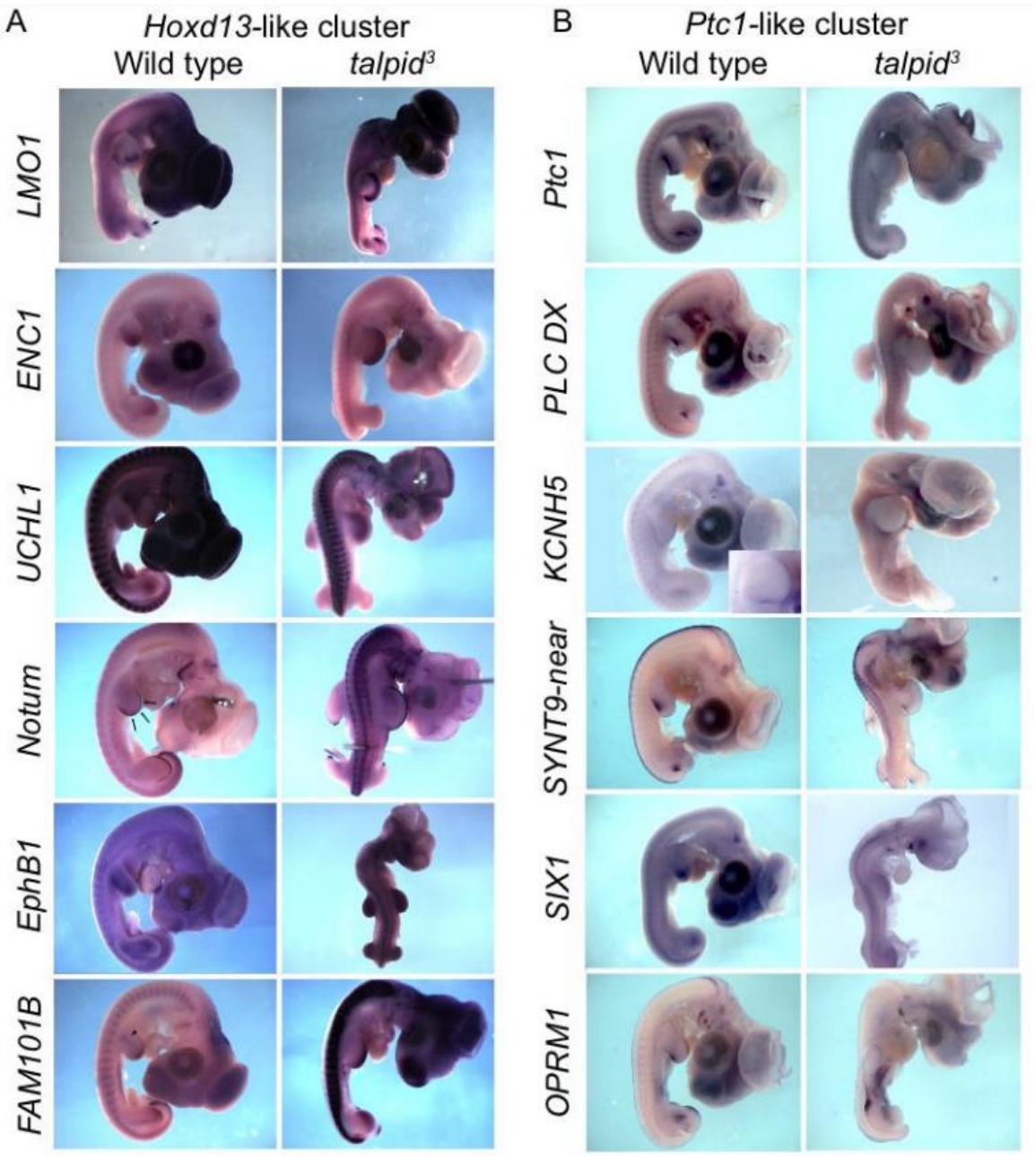
A
Hoxd13-like cluster
Wild type
talpid3
LMO1
ENC1
UCHL1
Notum
EphB1
FAM101B
B
Ptc1-like cluster
Wild type
talpid3
Ptc1
PLC DX
KCNH5
SYNT9-near
SIX1
OPRM1

Figure 4

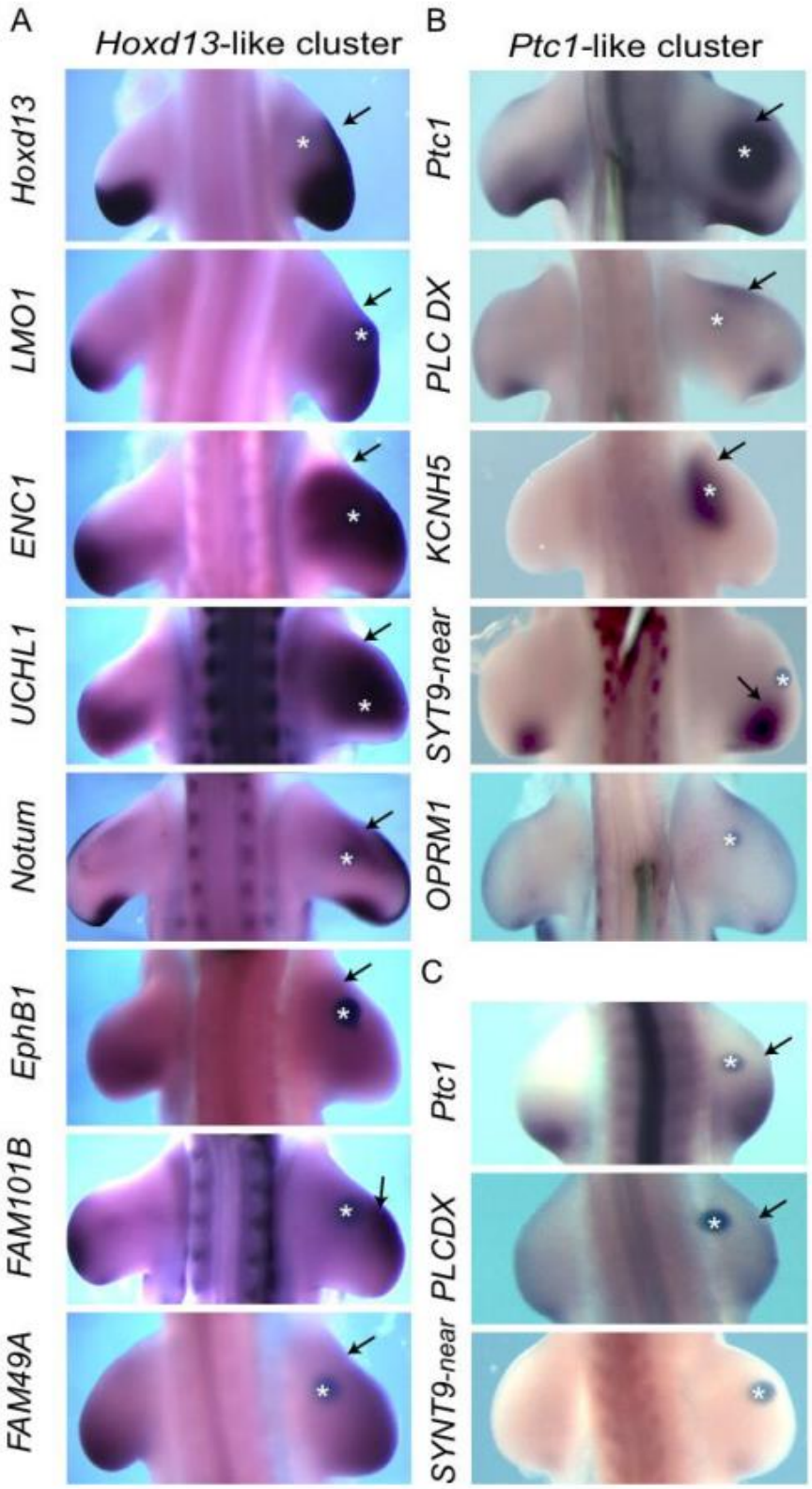
A
Hoxd13-like cluster
Hoxd13
LMO1
ENC1
UCHL1
Notum
EphB1
FAM101B
FAM49A
B
Ptc1-like cluster
Ptc1
PLC DX
KCNH5
SYT9-near
OPRM1
C
Ptc1
PLCDX
SYNT9-near

Figure 5

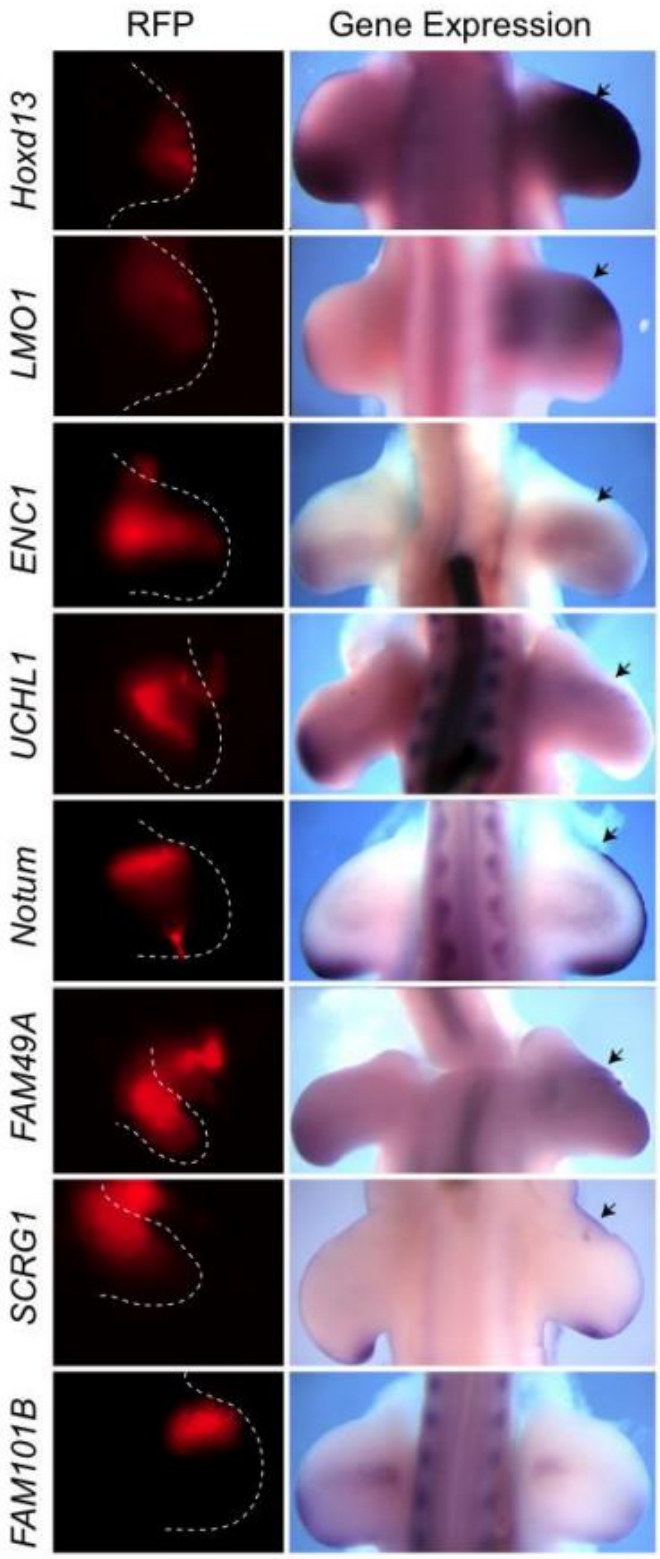
RFP
Gene Expression
Hoxd13
LMO1
ENC1
UCHL1
Notum
FAM49A
SCRG1
FAM101B

Figure 6

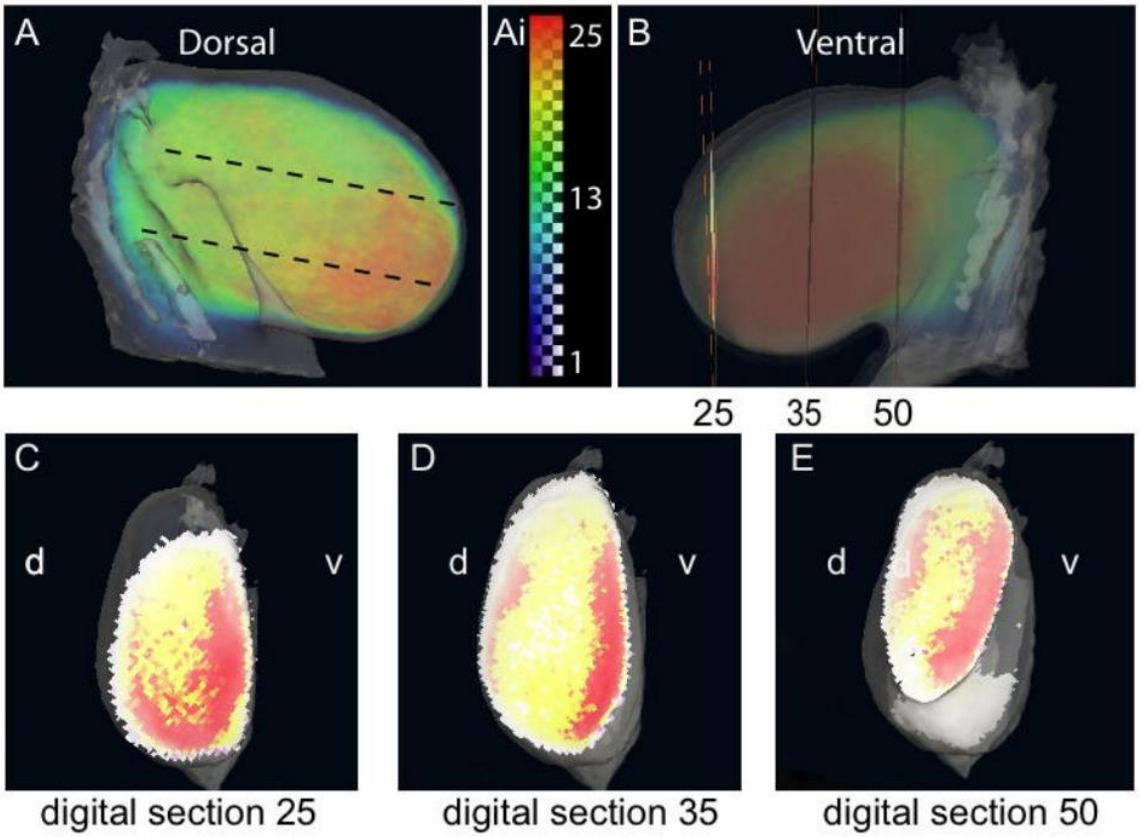
A
Dorsal
Ai
25
13
1
B
Ventral
25
35
50
C
d
v
digital section 25
D
d
v
digital section 35
E
d
v
digital section 50

Figure 7

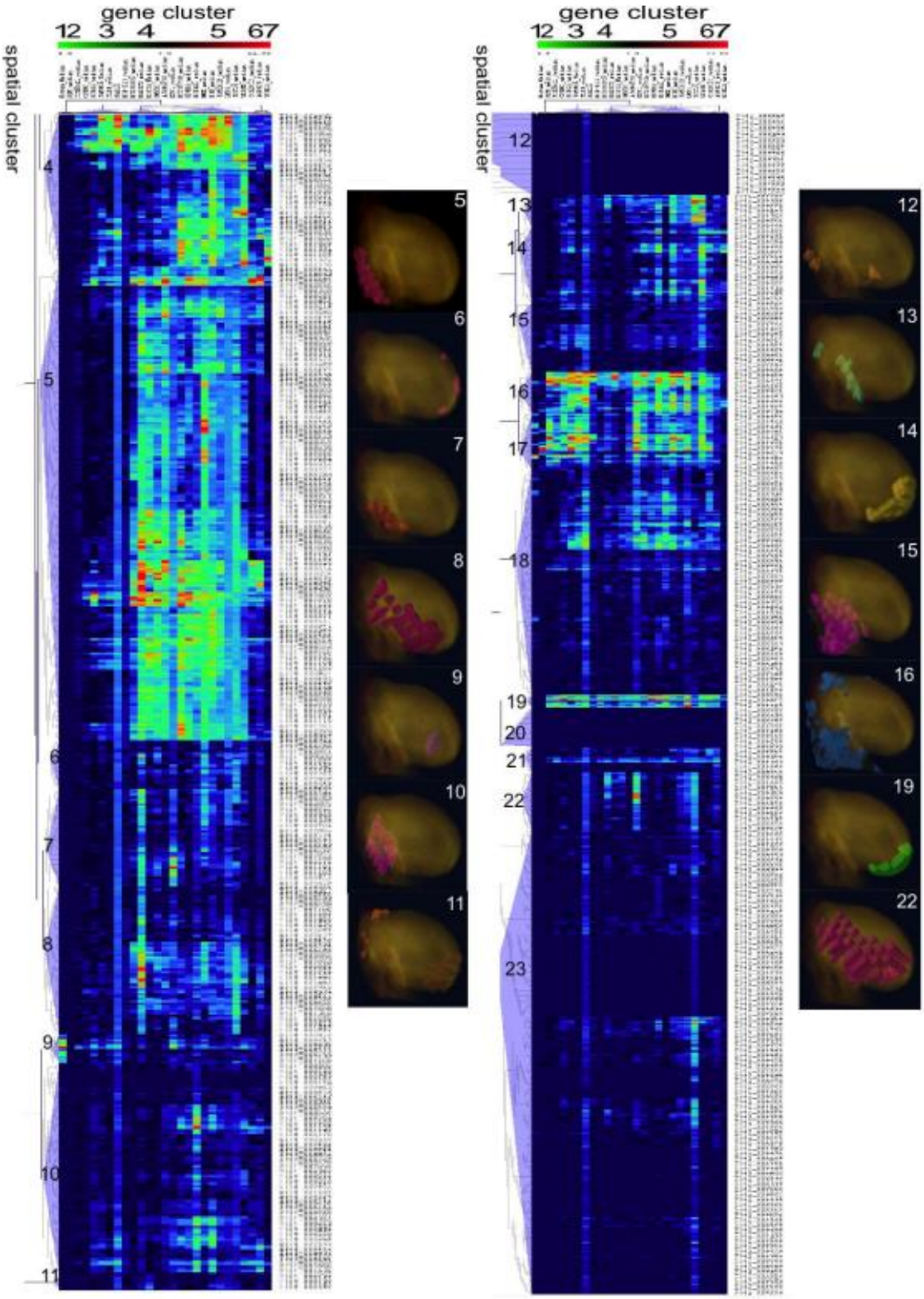
gene cluster
1 2 3 4 5 6 7
spatial cluster
4
5
6
7
8
9
10
11
5
6
7
8
9
10
11
gene cluster
1 2 3 4 5 6 7
spatial cluster
12
13
14
15
16
17
18
19
20
21
22
23
12
13
14
15
16
19
22

Figure 8

Cluster	Gene Name
1	**Notum** *
2	Shh
3	CPXM2
	TCERG1L
	TLE4
	SALL1
	Hoxd13
	SCRG1
	FAM49A
4	Novel transcribed locus BU388665
	RASSF3
	DOC2A
	SYMD2
	Known protein coding AJ444373
5	**LMO1**
	ENC1
	EphB1
	MMP
	BID
	FAM101B
	FSTL4
	Novel transcribed locus BU289700
	Hoxa11
	VEGFD
6	COLEC12
	AGPAT5
7	**UCHL1**

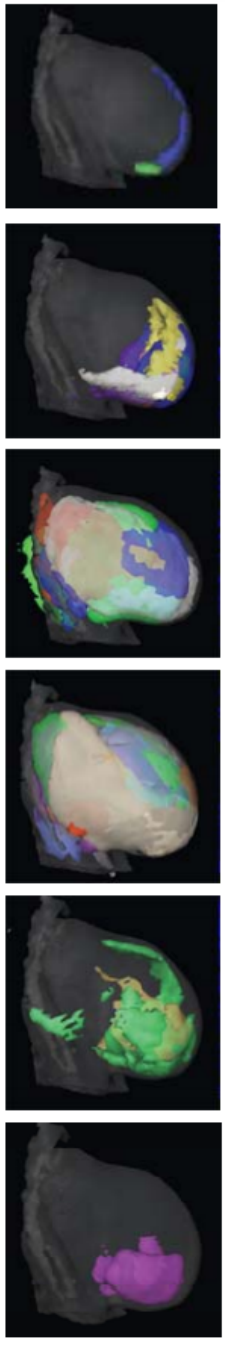

Table 1

Cluster	Gene Name
9 (24/26)	FAM49A
	TLE4
	TCERG1L
	Novel Transcribed locus BU388665
	RASSF3
	BID
	SYMD2
	COLEC12
	Novel transcribed locus BU289700
	FSTL4
	DOC2A
	AGPAT5
	MMP
	Known protein coding AJ444373
	CPXM2
	ENC1
	FAM101B
	SCRG1
	EphB1
	Sall1
	Hoxa11
	Hoxd13
	LMO1
	VEGFD
14 (23/26)	FAM49A
	TLE4
	TCERG1L
	Novel Transcribed locus BU388665
	RASSF3
	BID
	COLEC12
	Novel transcribed locus BU289700
	FSTL4
	DOC2A
	AGPAT5
	MMP
	Known protein coding AJ444373
	CPXM2
	ENC1
	FAM101B
	SCRG1
	EphB1
	Sall1
	Hoxa11
	Hoxd13
	LMO1
	VEGFD
19 (21/26)	FAM49A
	TLE4
	TCERG1L
	RASSF3
	BID
	COLEC12
	Novel transcribed locus BU289700
	FSTL4
	MMP
	Known protein coding AJ444373
	CPXM2
	ENC1
	FAM101B
	SCRG1
	EphB1
	Sall1
	Hoxa11
	Hoxd13
	LMO1
	Shh
	VEGFD
22 (23/26)	FAM49A
	TLE4
	Novel Transcribed locus BU388665
	RASSF3
	BID
	SYMD2
	COLEC12
	Novel transcribed locus BU289700
	FSTL4
	DOC2A
	AGPAT5
	MMP
	Known protein coding AJ444373
	ENC1
	FAM101B
	SCRG1
	EphB1
	Sall1
	Hoxa11
	Hoxd13
	LMO1
	VEGFD
	UCHL1